Engineering Geology 348 (2025) 107962

Contents lists available at ScienceDirect

Engineering Geology

journal homepage: www.elsevier.com/locate/enggeo

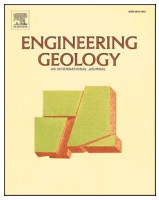

Spatial multi criteria analysis of ground conditions in early stages railway planning using analytical hierarchy process applied to viaduct-type rail in Southern Sweden.

Joakim Robygd [a,*], Lars Harrie [b], Tina Martin [a]

[a] Lund University, Faculty of Engineering, Department of Biomedical Sciences, Division of Engineering Geology, John Ericssons väg 1, Lund, Sweden
[b] Lund University, Physical Geography and Ecosystem Science, Sölvegatan 10, Lund, Sweden

ARTICLE INFO

Keywords:
Pier localisation
Suitability
Ground classification
Planning

ABSTRACT

This study applies a spatial multi-criteria analysis to assess ground suitability for pier-supported viaduct railways using the Analytical Hierarchy Process (AHP). By integrating expert judgments, the analysis evaluates six key geotechnical categories—soil type, soil depth, rock type, slope, wetness index, and groundwater occurrence—to map ground suitability. Three weight normalisation methods were tested to explore how different normalisation approaches affect the resulting suitability assessments. The results reveal significant variations in suitability maps, highlighting how different expert weighting strategies can influence decision-making during early-stage railway planning. Uncertainty maps were generated and used to identify areas requiring further investigation. The methodology is applied to an area in Southern Sweden, between the cities of Lund and Hässleholm to compare the weighting strategies over a relevant and geologically diverse area. A practical application comparing foundation types along identified routes showed that AHP-guided pathfinding achieved a clear preference for ground conditions suitable for non-piled foundations compared to a reference line. The method provides a systematic framework for preliminary geotechnical evaluations in railway planning, enabling more focused site investigations and supporting industrialized construction approaches.

1. Introduction

Geological site characterization is a crucial initial step in any land exploitation planning (Bell et al., 1987), particularly for large-scale infrastructure projects such as railways. This process involves a comprehensive assessment of subsurface conditions to ensure the safety, stability, and feasibility of the proposed development. Typically, site investigations for railway projects begin with a desktop study, which is followed by detailed field investigations. The desktop study synthesizes available data—often derived from geological, hydrogeological and topographical maps, aerial photography, and LiDAR scans—to provide an initial interpretation of ground conditions along the proposed railway line (Griffiths, 2017). These preliminary assessments provide the framework for subsequent field investigations, which are crucial for validating initial findings and establishing design parameters for identified geological units.

The importance of accurate ground condition assessments cannot be overstated, as they form the foundation of the entire planning process for new railways. For example, as discussed by Nowell (2021), the High-Speed 2 (HS2) railway project in Great Britain encountered significant delays and cost overruns due to insufficient geological investigations. The author emphasizes the critical role of up-to-date and high-quality geological maps in mitigating such risks. The practice of extended geological mapping, investigation, and interpretation in infrastructure projects is well-documented by Fookes and Baynes (2001) and Baynes et al. (2005). Their work highlights the necessity of thorough geological assessments to avoid unforeseen challenges during construction. Similarly, Huang et al. (2013) underscore the importance of precise geological characterization, particularly for linear infrastructures like railways. Their research focuses on identifying geological risk factors in the planning stages to prevent complications during construction.

However, the effectiveness of these preliminary investigations can vary significantly depending on the quality, quantity, and interpretation of the available data. The challenge lies not only in gathering this data but also in condensing it into a readable and understandable format that effectively communicates the underlying uncertainties.

* Corresponding author.
E-mail addresses: Joakim.robygd@tg.lth.se (J. Robygd), lars.harrie@nateko.lu.se (L. Harrie), tina.martin@tg.lth.se (T. Martin).

https://doi.org/10.1016/j.enggeo.2025.107962
Received 12 November 2024; Received in revised form 23 January 2025; Accepted 9 February 2025
Available online 14 February 2025

In Sweden, current ground characterization methodologies primarily focus on ballast embankment foundations, except where tunnels or bridges are required (Swedish Transport Administration, 2018). However, recent developments in railway construction, particularly in Asia, present alternative approaches with promising outcomes. The success of pier-elevated high-speed tracks in Japan's Shinkansen system (Koyama, 1997) and China's implementation of the China Railway Track System III Slab Ballastless Track (CRTS III sbt) demonstrate the viability of alternative construction methods with accelerated timelines (Su et al., 2019). As Sweden plans its next generation of railway lines (Government Office of Sweden, 2023), there is growing interest in exploring pier-supported viaduct-tracks as an alternative construction method.

Transitioning to pier-supported tracks represents a significant shift in ground loading patterns, moving from continuous to pointwise loads. Embankment construction requires extensive earth moving and consideration of cut-and-fill volumes along the entire railway corridor. However, pier-supported viaduct systems fundamentally alter this concept. Unlike continuous earthwork operations, pier foundations introduce discrete loading points at regular intervals, which considerably reduce the significance of mass balance considerations. However, these point loads place higher demands on the subgrade beneath the pier foundations (Nie et al., 2017). This shift in construction methodology requires a revised approach to ground characterization, emphasising localised ground conditions at pier locations rather than continuous corridor-wide earth volume calculations.

The proposed method for ground characterization relies on spatial multi criteria analysis (MCA). This approach has been used extensively throughout the literature and applied to several fields. In the fields of engineering geology, ground condition ranking has been the primary use case. Site characterization can be narrowly niched towards geological hazard, for example (Delmonaco et al., 2003; Skilodimou et al., 2019) or as suitability studies for a wide range of applications. As a way of condensing information into useable communications, geographical information systems (GIS) and computer-aided design (CAD) software are routinely used. GIS utilized for multi-criteria analysis have been applied to for example agricultural land use planning (Elsheikh et al., 2013), locating favourable areas for geothermal resources (Yalcin and Kilic Gul, 2017), predicting areas of sustainable groundwater resources (Adiat et al., 2012) and evaluating railway corridors based on ecological and geological factors (Karlson et al., 2016). However, all these studies are coupled to ground conditions.

One commonly applied MCA is the analytical hierarchical process (AHP). The method helps prioritize and evaluate options based on a hierarchy of criteria. It involves breaking down a complex decision into a series of pairwise comparisons between alternatives by ranking their relative importance on a predetermined scale. The results of the comparisons are aggregated to produce an overall ranking (Saaty, 2008). AHP has been applied successfully for geological and geotechnical suitability judgments (Deng et al., 2023; Costa et al., 2011) and provides an easy overview of the aggregated information related to the objective at hand. The AHP methodology was selected for this study due to its robust approach in deriving criteria weights through systematic pairwise comparisons and eigenvalue calculations. This method has been widely established in the literature for weight determination, offering transparency in capturing and synthesizing expert judgments (Ishak et al., 2019).

While extensive research exists on geological assessments for railway planning, there is room for improvement in applying these methods to specific construction techniques like pier-supported railway systems, particularly in the Swedish context. This study explores the application of a combined MCA-AHP and GIS approach to assess ground suitability for viaduct-type railways. The type of viaduct rail system considered here is prefabricated elements of 40 m in length produced in temporary factories along the build line. Therefore, once a line is determined, a smaller area every 40 m are subject for ground investigations. By comparing different weighting strategies and incorporating uncertainty analysis, our method aims to provide a more nuanced tool for early-stage railway planning. This approach contributes to ongoing discussions on geotechnical assessments and aims to contribute to enhance the efficiency and reliability of railway infrastructure development in Sweden and in other regions with similar geological contexts.

The overall aim of this study is to evaluate the suitability and effectiveness of the MCA-AHP methodology for early-stage ground suitability assessments in infrastructure planning. To achieve this, we apply the methodology to a study area in Sweden between the cities of Lund and Hässleholm, where complementary geological mapping has already been conducted (Fig. 1). This application serves to demonstrate the practical implementation of the method and assess its performance in a real-world context.

While the case study focuses on pier-supported viaduct railways, the approach is designed to be adaptable to various infrastructure projects requiring geoscientific evaluations. The study's objectives are fourfold:

1. To compute a map of ground suitability for pier foundations.
2. To evaluate the impact of different weighting strategies within the AHP method on the estimation of ground suitability.
3. To estimate the uncertainty in the suitability assessment.
4. Compare weighting methods in a practical use case for localisation based on ground suitability.

The following sections detail the study area characteristics, methodology, and weighting approaches, followed by results presentation and discussion. The paper concludes with a practical application case study and recommendations for future research.

2. Site description

The area selected for the study was chosen due to the diverse geology of the area and the fact that extended geological mapping is done over the area (Ising et al., 2019). For the method to be thoroughly tested, variations in ground conditions are favourable. The area spans over two main solid geology regions. One dominated by sedimentary bedrock cover and the other by Precambrian gneisses and granites (Fig. 1). The NE parts is dominated by crystalline bedrock with frequent dolerites cutting through in a predominately NW-SE direction. The SW side of the investigation area is dominated by limestones, sandstones and shales, typically displaying an undulating bedrock surface with thick Quaternary covers in the valleys. The bedrock surface of the crystalline region undulates at a smaller scale and soil depths are usually less (Ising et al., 2019).

The entire area was covered by the Weichselian ice sheet during the last glacial maximum at around 22,000 years ago (Stroeven et al., 2016). Based on geochronology by Anjar et al. (2013), deglaciation of the investigation area occurred around 17 ka ago. The NE part of the area was covered in glacial meltwater connected to the Baltic basin for a time while the rest of the area has been free from lake and/or marine incursions following the deglaciation. Glacial erosion and deposition have rendered the surface of the area sparse in deeply weathered rock and few areas of clay mineral deposits are present in surface layers. Exceptions exists in the area where subaerial kaolinite can be found in the NW part of the area (Ringberg, 1992). Glacial erosion of softer rocks such as the southern clay shales and limestones has given rise to fine grained till deposits, dominated by clay and usually over-consolidated through the subglacial depositional environment. In the crystalline areas due to the harder nature of the bedrock, sandy and gravelly glacial tills dominate. These coarser tills contain numerous large boulders, both at the surface and throughout the vertical profile. Glacial meltwater has produced erosional scars in the till, depositing esker-like deposits of sorted coarse-grained material, mostly present in the northern part of the area. Sorted fine grained material is only found as surface layers in local depressions such as river valleys and former ice-dammed lakes, although older deposits of sorted fines covered by till have been documented (Ringberg,

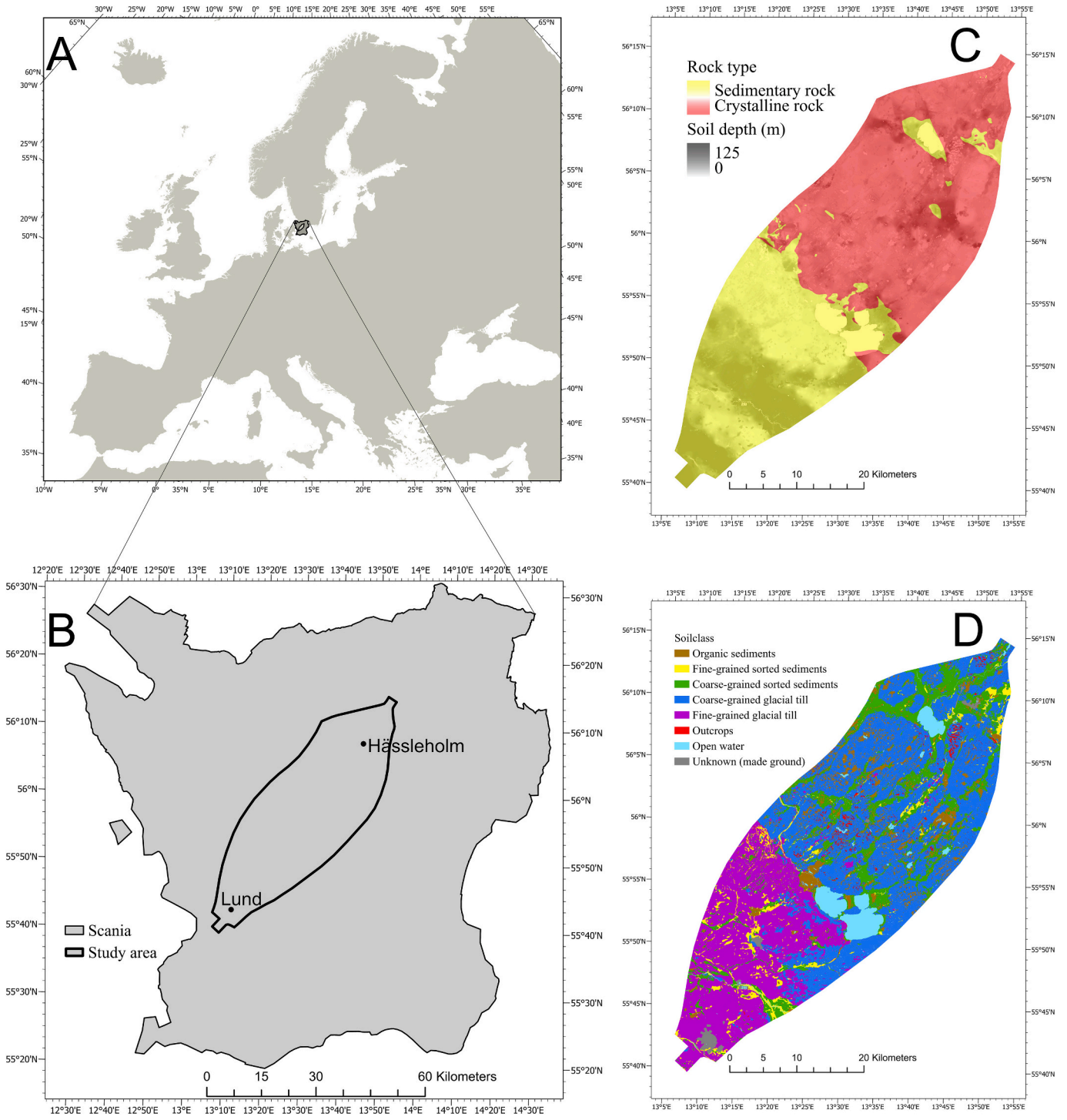

Fig. 1. A & B) Geographical location of the study area within Europe and Scania. C) rock type domains of crystalline (red) and sedimentary rocks (yellow). The shading from transparent to dark showcases the depth to bedrock where transparent indicates shallow depth and dark hues indicate deep soil depths. D) Soil type distribution over the area. Note the close relationship between fine-grained tills (purple) with sedimentary bedrock in B and coarse-grained tills (blue) with crystalline bedrock.

1992). Organic deposits are common within the whole area while rock outcrops are only common in the central and NE half of the area.

The coarse-grained glacial tills vary between domination of sand and gravel where sand is the most common dominating grain size. The coarse-grained tills in the area are described as less consolidated dead-ice deposits with a normal frequency of boulders. The fine-grained tills are of two main varieties, one more clay-rich, less consolidated and one less clay-rich, over-consolidated with significant amounts of sand and gravel. The latter is usually found below the former in the southernmost part of the area (Ringberg, 1992). All glacial tills are expected to carry larger boulders, although less in the clay-rich tills. Technical parameters for the two fine-grained glacial till units are well documented from the literature and various projects (Larsson, 2000; Larsson, 2001; Dueck, 1998; Malmborg, 1983) and are ascribed an effective friction angle of about 20–32°. The coarse-grained tills are shown to have a friction angle of between 35° and 45° depending on the

pre-consolidation pressure (Larsson, 1989). In this area where the coarse tills predominately are deposited as dead-ice melt-out tills, the friction angle should be within the range 35° to 38°.

3. Methodology

Criteria for early mass balance estimations in a classical embankment-type case are focused on the type of soil and rock present and its geometry (Swedish Transport Administration, 2018). The soil types are classified based on their common mechanical properties and volume of shifted masses can be estimated conveniently based on projected and true elevation of the landscape. The pointwise approach can be less concerned with this notion of planning due to the significantly smaller volumes of mass shifting required during construction. Instead, aspects of ease of construction can be evaluated to best determine suitable locations of pier placements. Based on a set of standardized foundation types, the ground conditions may present unique challenges during construction depending on the conditions outlined below.

3.1. Category selection

To compute the ground suitability for the pier foundations six main categories are used: soil type, soil depth, rock type, wetness index, slope and groundwater occurrence. For each category a number of subcategories are defined (Table 1). The relevance of the used categories is summarized below:

3.1.1. Soil type

The soil type criteria describe the unconsolidated material on which the pier foundations are to be constructed. The soil type decides material properties such as porosity, permeability, bearing capacity, shear strength and compressibility of the sub-foundation material. The aggregation of several soil types into larger groups was necessary to keep an overview in the pairwise comparison stage. The aggregation of soil types into classes is similar to the one developed by the Swedish Geotechnical Institute (SGI, 2016) which are geotechnical terrain classes based on the soil type's mechanical properties. The aggregation was adapted to the investigation area. See Table 1 for full overview of subcategories.

Table 1
List of all main categories used in the study. For all main categories a fixed number of values are allowed, in this paper denoted subcategories.

Soil type	Soil depth	Rock type	Wetness index	Slope	Groundwater occurrence
Fine grained glacial tills	0–3 m	Sedimentary bedrock	Dry	0–5 °	Fracture aquifer, Small
Coarse grained glacial tills	3–11 m	Crystalline bedrock	Moist	5–10 °	Fracture aquifer, Large
Sorted coarse grained material	11–24 m		Wet	10–18 °	Porous aquifer, Small
Sorted fine grained material	24–46 m		Discharge	>18 °	Porous aquifer, Large
Unknown (made ground)	>46 m				
Organic sediment					
Open water					

3.1.2. Soil depth

For pier-supported structures, soil depth has critical implications for the foundation design. The soil depth criteria have a twofold meaning. First, it determines the foundation type selection (shallow or deep foundations) and construction approach at each pier location, including excavation requirements if the near-surface material is unsuitable for the concentrated loads. Secondly, greater soil depths typically indicate more complex stratigraphy, suggesting the need for detailed site-specific investigations to understand potential bearing layer characteristics and pile design requirements.

3.1.3. Rock type

The type of rock becomes important where soil depths are shallow, and foundations may be constructed on consolidated material. The specific rock type is not considered here, instead a distinction is made between sedimentary rocks and crystalline rocks where the latter comprises both igneous and metamorphic rocks. The recent glacial erosion in the area generally means that deeply weathered rock is uncommon whereby this distinction can be made purely based on best/worst case loading capacity which differs significantly between sedimentary and crystalline rocks in the absence of deep chemical weathering horizons.

3.1.4. Wetness index

The wetness index describes the surface wetness of the ground over most of the year. This index can be argued to indicate the risk of flooding and thereby seasonal erosion, the ground materials permeability as well as vertical proximity to shallow groundwater. These indirect indices can have implications for both the long-term stability of foundations as well as measures taken during construction.

3.1.5. Slope

The slope criteria is directly linked to the shifting of masses. Since each individual foundations are to be constructed on level ground, sloping ground needs to be amended by excavation and/or backfilling.

3.1.6. Groundwater occurrence

The groundwater criteria is based on the larger defined aquifers in the area. The relevance to the suitability is related to material infiltration capacity and need for pumping systems during open shaft earth works. The grouping was based on type of aquifer (in unconsolidated or consolidated material) and the groundwater potential. For large porous aquifers, more than 5 l/s is available and for large fracture aquifers, more than 5.5 l/s.

A nested category regarding natural hazards should be included in the judgement if deemed necessary for the investigated area, for example as described by Bathrellos et al. (2017). The example area covered in this article is tectonically stable (Joshi et al., 2024). and mostly above the highest postglacial marine limit (Anjar et al., 2013) which is the primary depositional environment for quick clays that are considered prone to landslides (Andersson-Sköld et al., 2013). In landslide prone areas, methodologies such as exposure mapping along the investigated area can be readily incorporated (Marchesini et al., 2024). However, there is the risk of flooding events around the lakes in the area, but they are not akin to flash flood events and have little bearing on pier elevated structures. If flooding risk is crucial for the evaluation in a specific area, flooding hazards can be evaluated separately using the AHP method, e.g. Fernández and Lutz (2010).

The proposed methodology requires certain minimum data inputs but is designed to be adaptable to different contexts and data availability. Essential data requirements include:

- Basic geological mapping (soil and rock types).
- Soil depth or depth-to-bedrock estimates.
- Topographical data for slope analysis.
- Groundwater or hydrogeological information.

This study utilizes high-resolution Swedish geological survey data, but the methodology can be implemented with different data resolutions and sources. For example, soil type classifications can be adapted to local geological contexts and classification systems for the pier foundations used. Where detailed soil depth measurements are unavailable, geophysical surveys or borehole interpolations can provide adequate estimates. The criteria selection process should reflect both data availability and local geological challenges. For instance, regions with significant seismic activity might incorporate additional stability-related criteria, while areas with extensive karst development might require specific subsurface void assessment criteria.

Numeric parameters (soil depth and slope) were divided into intervals. The first interval was based on logical assumptions of ideal conditions. For the remaining intervals, K-means clustering (Jain, 2010) was employed, a statistical method that groups data points into a specified number of clusters. To determine the optimal number of clusters, the elbow method (Shi et al., 2021) was utilized. This method involves plotting the within-cluster sum of squares (WCSS) against the number of clusters and identifying the 'elbow' point where the rate of decrease sharply shifts, indicating diminishing returns for additional clusters.

3.2. Data

Data used are only open data which are freely available to anyone. More detailed underground data from geotechnical soundings and drillings are not yet available to the public and exists on private company servers or locked into proprietary file-formats. While such data would have been useful, the analysis aims to be easily tested and compared with other expert groups, so open data sets are ideal. All the data was processed to populate the points in a 10-m grid covering the study area. Polygon data were rasterized to the common resolution and higher resolution rasters were resampled through nearest neighbour interpolation. The data sources are outlined in Table 2.

Table 2
Data sources of the used categories. The data is freely available either directly or through processing of freely available data.

Criteria	Description	Scale	Data source
Soil type	Polygons of soil types obtained from aerial analysis, field mapping and terrain analysis by Swedish geological survey (SGU).	1:25,000	https://resource.sgu.se/data/oppnadata/jordarter 25 k–100 k/jordarter25 k–100 k.zip
Soil depth	GeoTiff representing depth to bedrock based on well data and outcrop observations from the soil type layer.	10 × 10 m	https://resource.sgu.se/data/oppnadata/jorddjupsmodell/jorddjupsmodell.zip
Rock type	Polygons and polylines of bedrock information. Only the field denoting rock type used here.	1:50,000–1:250,000	https://resource.sgu.se/data/oppnadata/berggrund 50 k–250 k/berggrund50 k–250 k.zip
Wetness index	Raster data of classed ground surface wetness. Based on LIDAR scans and topographic and geological information through a predictive model.	2 × 2 m	Ågren, A.M., Larson, J., Paul, S.S., Laudon, H. and Lidberg, W., 2021. Use of multiple LIDAR-derived digital terrain indices and machine learning for high-resolution national-scale soil moisture mapping of the Swedish forest landscape. Geoderma, 404, p.115280.
Groundwater occurrence	Polygons and polylines describing groundwater reservoirs.	1:50,000–1:250,000	https://resource.sgu.se/data/oppnadata/grundvattenmagasin/grundvattenmagasin.zip
Slope	Derived from DEM 2 × 2 meters.	2 × 2 m	Swedish mapping, cadastral and land registration authority

3.3. Expert judgments using AHP method

Analytical hierarchy process involves pairwise comparisons to establish priorities among categories and sub- categories, assigning weights based on their relative importance. The method provides synthesis of qualitative and quantitative data, making several data types suitable. The final product after category-based weighting is an index of ground suitability for pier foundation construction. The task is therefore to define a suitability index (y) for each cell in a raster. This index is defined under the assumption that: (1) for each cell there is a value in the list of subcategories for each main category, and (2) the index is dependent on the subcategory values (according to a weight) and that the subcategory values are independent of each other. Hence, the suitability index is defined as a linear combination:

$$y = \sum_{i=1}^{n} w_{t_{i,j}} \quad (1)$$

where $w_{t_{i,j}}$ is the weight for subcategory j for the main category i, and n is the number of main categories (which in this study is equal to six, see Table 1). It should be noted that for each cell in the raster there is only one sub-category value for each main category (for each cell).

This implies that we need to define the weights for the subcategories. In this study we apply the AHP method as a basis for the weighting. This method relies on expert judgments of the importance of each category and subcategory.

A total of six domain experts were asked to complete the pairwise comparisons of judgement matrices in the AHP process. The experts range from academic professionals to industry professionals at PhD education level within slightly different edge expertise in geology, engineering geology, hydrogeology and soil and rock mechanics. Each participant was asked to complete the pairwise comparison separately using the 1–9 judgement scale proposed by Saaty (1987). The participants used a template which automatically filled in the reciprocals and displayed a binary message upon matrix completion about consistency. If input was not consistent, participants were prompted to look over their response and edit their input if deemed reasonable. The main criteria matrix was first to be judged, and participants had full overview of the subcategories contained in each main criteria to better be able to complete a meaningful pairwise comparison. Each sub-criteria matrix was subsequently judged in the same way.

For each pair of a category, a pairwise comparison is filled out by the elicited expert to determine their relative importance. This is done by assigning a numerical value a_{ij} using the predefined scale (Table 3), where:

$a_{ij} = 1$ indicates that category C_i and C_j are equally important.
$a_{ij} > 1$ indicates that C_i is more important than C_j.
$a_{ij} < 1$ indicates that C_i is less important than C_j.

The elements in the judgement matrix is a positive reciprocal matrix **A** with the following properties:

Table 3
Ranking scale for pairwise comparison.

Scale	Description
1	Equal importance
3	Moderate importance
5	Strong importance
7	Very strong importance
9	Extreme importance
2, 4, 6, 8	Intermediate values between adjacent numbers
1/n	Inverse values for the corresponding numbers

$$A = \begin{bmatrix} 1 & a_{1,2} & \dots & a_{1,n} \\ {}^{1}/_{a_{1,2}} & 1 & \dots & a_{2,n} \\ \dots & \dots & \dots & \dots \\ {}^{1}/_{a_{1,n}} & {}^{1}/_{a_{2,n}} & \dots & 1 \end{bmatrix}, \quad a_{k,l} > 0 \forall k,l = 0,1,2,\dots,n \tag{2}$$

where n is the number of main categories.

The result of all of the subcategories can also be formulated in judgement matrixes (e.g.$\mathbf{B}_i$for the main category i) are of similar forms:

$$B_i = \begin{bmatrix} 1 & b_{1,m_j} & \dots & b_{1,m_j} \\ {}^{1}/_{b_{12}} & 1 & \dots & b_{2,m_j} \\ \dots & \dots & \dots & \dots \\ {}^{1}/_{b_{1,m_j}} & {}^{1}/_{b_{2,m_j}} & \dots & 1 \end{bmatrix} \text{ and } b_{k,l} > 0 \forall k,l = 0,1,2,\dots,m_i \tag{3}$$

where m_i is the number of subcategories for the main category i.

After completion of individual judgement matrixes, the experts all convened for discussions on an agreed upon common judgement matrix of the main criteria. Sub-criteria matrices were determined by aggregation of individual judgments using the weighted geometric mean of all answers. The difference in creating the final judgement matrices in main criteria and sub-criteria was due to the time-consuming nature of the expert discussions and the proven reliability of the aggregation consensus (Krejčí and Stoklasa, 2018). The choice to use a judgement scale with crisp numbers instead of fuzzy relied on the premise to simplify and minimize the required efforts of the individual experts, i.e. for practical implementation purposes.

3.4. Calculating the weights in the AHP method

3.4.1. Weighting the main categories

The weights of the properties in the judgement matrix can be estimated using the eigenvector method (Saaty, 1987). Assume that $\lambda_{\max}$is the largest eigenvalue for the judgement matrix **A** and that$\mathbf{e}_{\max}$is the corresponding eigenvector, i.e.:

$$Ae_{max} = \lambda_{max} e_{max} \tag{4}$$

Then, the normalized eigenvector$\mathbf{w}_{mc}$includes the weights for the different properties of the main categories (w_{mc_i}), that is:

$$w_{mc} = [w_{mc_1} \;\; w_{mc_2} \;\; \dots \;\; w_{mc_n}] = \frac{[e_{max_1} \;\; e_{max_2} \;\; \dots \;\; e_{max_n}]}{\sum_{i=1}^{n} e_{max_i}} \tag{5}$$

where $e_{max_i}$is the i:th value in the eigenvalue vector.

3.4.2. Weighting of the subcategories

In our study we put the final weights on the subcategories level. For example, what is the weight of the subcategory *Fine grained sill* (that is part of the main category *Soil type*). The weight of the subcategories should be based on both the importance of the main category (described by the weights w_{mc_i}) as well as the relative importance of the subcategory in comparison with other subcategories within the same main category. As input to the latter we can use the judgement matrixes for the subcategories (denoted **B**, see 2.4). However, it is not obvious how the weights of the subcategories should be defined; In this study we design, implement and evaluate three approaches to define the weights for features in the subcategory levels.

3.4.2.1. Method 1 (M1): weighting based on the eigenvector method. The weighting of the subcategories can be performed using the same method as for the main categories. These subcategory weights (for main category i and subcategory j) are denoted $w_{sc_{i,j}}$ below. This implies that we obtain the following:

$\mathbf{B}_i\mathbf{e}_{sc_i} = \lambda_{max}\mathbf{e}_{sc_i}$ and $\mathbf{w}_{sc_i} = [w_{sc_{i,1}} \;\; w_{sc_{i,2}} \;\; \dots \;\; w_{sc_{i,m}}]$ is the normalized value of $\mathbf{e}_{sc_i}$

Then, the total weight for a subcategory j under the main category i $(w_{t_{i,j}})$is:

$$w_{t_{i,j}} = w_{mc_i} w_{sc_{i,j}} \tag{6}$$

3.4.2.2. Method 2 (M2): weighting method to keep the relative weights of the main categories. One disadvantage with the eigenvalue method to define the weights (eq. 4) is that the total weight for a subcategory is decreasing if there are several subcategories for the same main category. This can be illustrated by the following example referring to Fig. 1 and Table 2. In the study we use more soil types than bedrock types. This implies that the weights for the soil type subcategories (*Coarse grained glacial till*, *Fine grained glacial till*, etc.) get comparatively smaller than the weights for the bedrock types (*Crystalline* and *Sedimentary bedrock*), which will violate the relative importance between the main categories (here Soil type and Bedrock type) as defined by the judgement matrix A and the weights.

To overcome the problem that the number of subcategories is affecting the total weights, we can adjust the weights of the subcategories. To ensure that the total weights of the subcategories does not affect the weight on the main categories we can state the condition that:

$$\prod_{j=1}^{m_i} \overline{w}_{s_{i,j}} = 1 \tag{7}$$

where $\overline{w}_{sc_{i,j}}$is the weight for subcategory feature i in main category j. That is, we get the following adjustment of the weights of the subcategories:

$$\overline{w}_{sc_{i,j}} = \frac{w_{sc_{i,j}}}{\sqrt[m_i]{\prod_{k=1}^{m_i} w_{sc_{i,k}}}} \tag{8}$$

Setting the weights according to eq. 8 guarantees that that the product of the weights for all subcategories (for a main category) is constant, which is shown by:

$$\prod_{j=1}^{m_i} \overline{w}_{sc_{i,j}} = \prod_{j=1}^{m_i} \frac{w_{sc_{i,j}}}{\sqrt[m_i]{\prod_{k=1}^{m_i} w_{sc_{i,k}}}} = \frac{\prod_{j=1}^{m_i} w_{sc_{i,j}}}{\left(\sqrt[m_i]{\prod_{k=1}^{m_i} w_{sc_{i,k}}}\right)^{m_i}} = \frac{\prod_{j=1}^{m_i} w_{sc_{i,j}}}{\prod_{k=1}^{m_i} w_{sc_{i,k}}} = 1 \tag{9}$$

Then, the total weight for a subcategory feature j for main category i $\left(\overline{w}_{t_{i,j}}\right)$is:

$$\overline{w}_{t_{i,j}} = w_{mc_i} \overline{w}_{sc_{i,j}} \tag{10}$$

3.4.2.3. Method 3 (M3): weighting method to include the relative distribution of features in the subcategories. The M2 method compensates for the number of subcategories, but it does not compensate for the relative distribution of features in the subcategories. An effect of this can be illustrated by the slope category in this study. As can be seen in Fig. 2

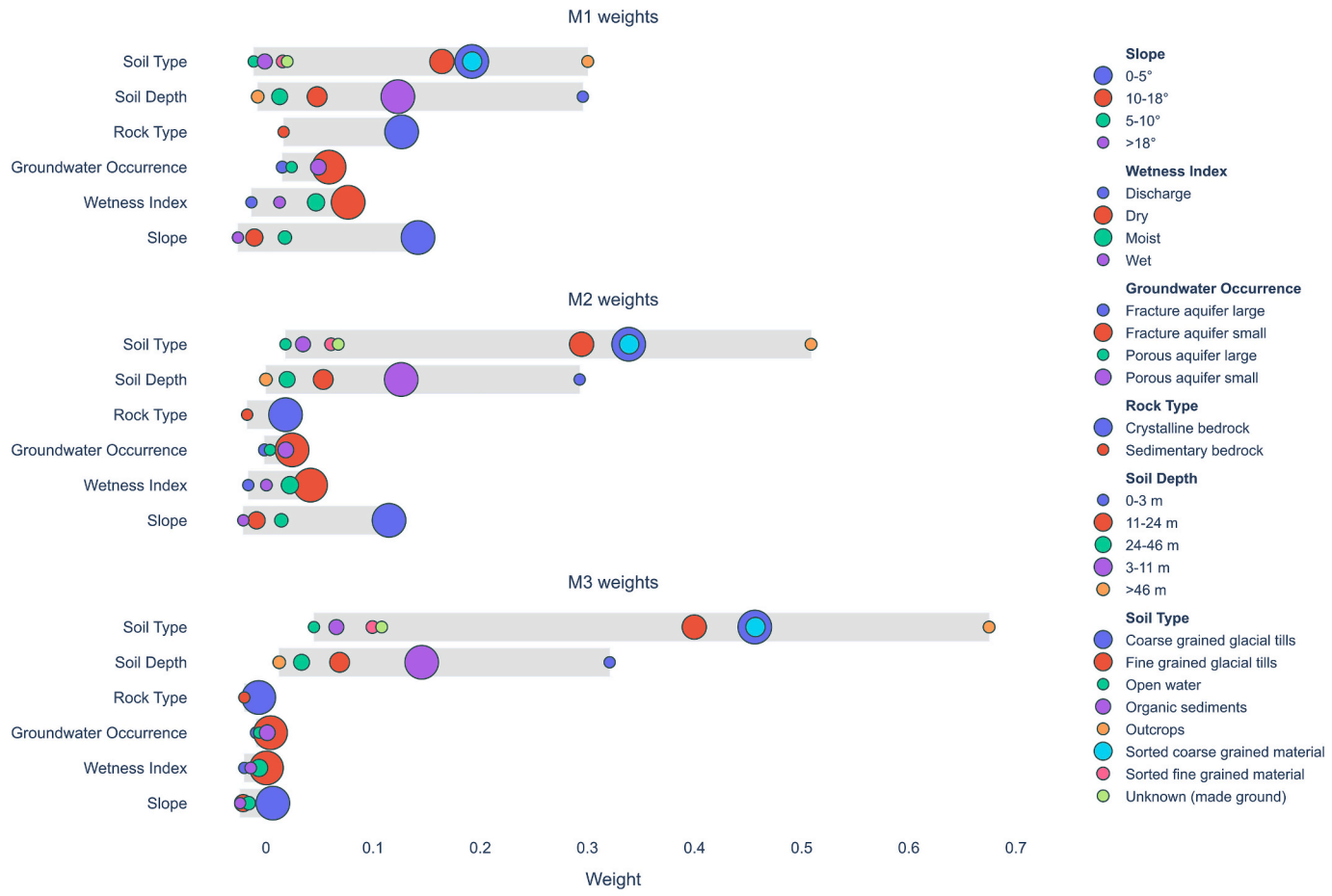

Fig. 2. Normalized weights of subcategories for each main category and method and their frequency in space. The size of each circle represents the frequency with which it occurs in the spatial data where a small radius implies low frequency and vice versa.

most observations in this category are within the most suitable sub-category ($0–5^0$). This implies that the slope category will have a substantial contribution to most suitability index values in method M1 and M2. A question here arises how the experts judge when they decided the relative importance of the main category, did they want the slope to have such a large influence of the suitability influence?

The purpose of M3 is to compensate for the distribution of the property values within each category. To facilitate this, we need to incorporate the property values into the computation of the weights. Assume that we have a study area **L** where the geotechnical investigations are performed. Within this study area there are q cells which have been investigated separately in terms of geotechnical properties. The total values for all cells in the study are$(L_{sum_i})$for main category (i) is then:

$$L_{sum_i} = \sum_{p=1}^{q} w_{t_{ip}} \tag{11}$$

where $w_{t_{ip}}$ is the total weight for the main category i in cell p.

Coming back to how the experts' judgement in the weight setting of the main categories. One possible way to judge is that the total weight value of the cells (L_{sum_i})should be relatively the same size as the weight for the main category w_{mc_i}. Applying this argument, we can define a normalized total weight $(\overline{\overline{w}}_{t_{i,j}})$ as:

$$\overline{\overline{w}}_{t_{i,j}} = f_i w_{t_{i,j}} \tag{12}$$

where the normalisation factor for the subcategory is given by

$$f_i = \frac{w_{mc_i} \Big/ \sum_{k=1}^{n} w_{mc_k}}{L_{sum_i} \Big/ \sum_{k=1}^{n} L_{sum_k}} = \left\{ \sum_{k=1}^{n} w_{mc_k} = 1 \right\} = \frac{w_{mc_i}}{L_{sum_i} \Big/ \sum_{k=1}^{n} L_{sum_k}} \tag{13}$$

We can study the effect of eq. 12 and 13, again using the slope category as an example. Since most of the slope properties were in the suitable sub-category ($0–5^0$), the L_{sum}value (as defined in eq. 11) for the slope category get large. This implies that the denominator in eq. 13 get large and hence the f_i and $\overline{\overline{w}}_{t_{i,j}}$(for the slope category) get small. This effect is illustrated in Fig. 2.

3.4.2.4. Normalisation of the weights for the subcategories. The absolute values for the weights of the subcategories $(w_{t_{i,j}}, \overline{w}_{t_{i,j}}$ and $\overline{\overline{w}}_{t_{i,j}})$ to compute the suitability index (eq. 1) are not interesting; what is important is the relative size of the weights between the categories. Therefore, we can rescale the weights to facilitate comparison between the three weighting strategies. This is performed by introducing rescaled weights, denoted $w^{rs}_{t_{i,j}}$for the first weighting method, that provides suitability values y^{rs}between 0 and 1. To derive the values for the rescaled weights we identify that:

$$\begin{aligned} y^{rs} &= \frac{y - y_{min}}{y_{max} - y_{min}} = \frac{y}{y_{max} - y_{min}} - \frac{y_{min}}{y_{max} - y_{min}} = \alpha y - \beta = \{eq.1\} \\ &= \alpha \sum_{i=1}^{n} w_{t_{i,j}} - \beta = \sum_{i=1}^{n} \left(\alpha w_{t_{i,j}} - \frac{\beta}{n} \right) = \sum_{i=1}^{n} w^{rs}_{t_{i,j}} \end{aligned} \tag{14}$$

where we denote the smallest suitability index y_{min} and the largest

y_{max} (using the original weights $w_{t_{i,j}}$), and $\alpha = \frac{1}{y_{max}-y_{min}}$ and $\beta = \frac{y_{min}}{y_{max}-y_{min}}$. Hence, we obtain:

$$w^{rs}_{t_{i,j}} = \alpha w_{t_{i,j}} - \frac{\beta}{n} \tag{15}$$

This is then repeated for the other weights (eq. 10 and eq. 12). The rescaled weights for the subcategories are denoted: $w^{rs}_{t_{i,j}}, \overline{w}^{rs}_{t_{i,j}}$ and $\overline{\overline{w}}^{rs}_{t_{i,j}}$.

3.5. Uncertainty estimations of the suitability map

From the expert interviews we received several judgement matrixes. Based on these matrixes we could estimate to which degree the experts agreed on the influence of the different (sub-) categories for the geotechnical suitability of pier foundation constructions. Based on the uncertainty in the judgement matrix we can estimate the uncertainties in the weight setting, and finally the uncertainty in the rescaled suitability maps (where the suitability values are between 0 and 1). The starting point for this analysis is an estimation of the uncertainties of the total weights $\left(\widehat{\sigma}_{w^{rs}_{t_{i,j}}}\right)$ for the first weighting method. This can be estimation by a combination of eq. 15 and eq. 6:

$$w^{rs}_{t_{i,j}} = \alpha w_{mc_i} w_{sc_{i,j}} - \frac{\beta}{n} \tag{16}$$

and the propagation law of uncertainties, i.e. we obtain:

$$\sigma_{w^{rs}_{t_{i,j}}} = \alpha \sqrt{w^2_{mc_i}\,\sigma^2_{w_{sc_{i,j}}} + w^2_{sc_{i,j}}\,\sigma^2_{w_{mc_i}}} \tag{17}$$

To estimate the uncertainties $\left(\widehat{\sigma}_{w^{rs}_{t_{i,j}}}\right)$ we perform the following steps:

1) Firstly, we estimate the uncertainties for the weights of the main category $\left(\sigma_{w_{mc_i}}\right)$ as well as the uncertainties for the weights of the subcategories $\left(\sigma_{w_{sc_{i,j}}}\right)$. These estimations are performed using a Monte Carlo (MC) simulation approach with 100,000 iterations to generate perturbed pairwise comparison matrices (**A** and **B**). This approach allows for simulating a range of potential judgement matrices based on input parameters derived from actual filled-in matrices. The random generation takes in the logarithm of the geometric mean of actual pairwise comparison matrices as a representation of the central tendency of judgments. The standard deviation of the actual pairwise comparisons capture the variability of the judgments. The logarithm of the geometric mean is perturbed by random values drawn from a normal distribution with the calculated standard deviation. The generated matrices are held reciprocal by only varying the triangle above the diagonal and calculating the reciprocals for the lower triangle. Through the generation process, consistency of the generated matrices is checked using the consistency ratio (CR), and only matrices with CR < 0.1 are saved for further analysis. It should be noted that this process has to be performed independently for the comparison matrix for the main category (**A**) and all the matrices for the subcategories ($\mathbf{B}_i$)
2) Based on the outcome of the MC simulations for the main category we estimate the uncertainties $\left(\widehat{\sigma}_{w_{mc_i}}\right)$. These uncertainties are estimated as:

$$\widehat{\sigma}_{w_{mc_i}} = \sqrt{\frac{\sum_{k=1}^{m}\left(\widetilde{w}_{mc_{i_k}} - w_{mc_i}\right)^2}{l}} \tag{18}$$

where $\widetilde{w}_{mc_{i_k}}$ is the k:th value of the weight estimated in the MC simulation, and l is the number of estimations in the MC simulation. Similarly, to estimate the uncertainties of the weights for the subcategories $\left(\widehat{\sigma}_{w_{sc_{i,j}}}\right)$ the following is conducted:

$$\widehat{\sigma}_{w_{sc_{i,j}}} = \sqrt{\frac{\sum_{k=1}^{l}\left(\widetilde{w}_{sc_{i,j_k}} - w_{sc_{i,j}}\right)^2}{l}} \tag{19}$$

where $\widetilde{w}_{sc_{i,j_k}}$ is the k:th value of the weight estimated in the MC simulation. Finally, the estimated uncertainties of the total weight are given by (cf. eq. 16):

$$\widehat{\sigma}_{w^{rs}_{t_{i,j}}} = \alpha \sqrt{w^2_{mc_i}\,\widehat{\sigma}^2_{w_{sc_{i,j}}} + w^2_{sc_{i,j}}\,\widehat{\sigma}^2_{w_{mc_i}}} \tag{20}$$

3) The uncertainty for the suitability index $\left(\widehat{\sigma}_y\right)$ of each cell in the raster is estimated from the propagation law of uncertainties:

$$\widehat{\sigma}_y = \sqrt{\sum_{i=1}^{n}\left(\frac{\delta y}{\delta w^{rs}_{t_{i,j}}}\right)^2 \widehat{\sigma}^2_{w^{rs}_{t_{i,j}}}} = \left\{\frac{\delta y}{\delta w^{rs}_{t_{i,j}}} = 1, \text{see eq.1}\right\} = \sqrt{\sum_{i=1}^{n}\widehat{\sigma}^2_{w^{rs}_{t_{i,j}}}} \tag{21}$$

where j is equal to the value for the subcategory for the main category i for that particular cell, and n is the number of main categories.

Above the uncertainty estimations for the suitability maps is specified for the first method to estimate the weights of the sub-categories $\left(w^{rs}_{t_{i,j}}\right)$. But the same approach could be applied to estimate the uncertainty with the other two methods for computing the weights $\left(\overline{w}^{rs}_{t_{i,j}}, \overline{\overline{w}}^{rs}_{t_{i,j}}\right)$. There are two things that differ. The first thing is the weights in eq. 19, that for method 2 becomes (cf. eq. 8):

$$\widehat{\sigma}_{\overline{w}_{sc_{i,j}}} = \sqrt{\frac{\sum_{k=1}^{l}\left(\frac{\widetilde{w}_{sc_{i,j_k}} - w_{sc_{i,j}}}{\sqrt[m_i]{\prod_{k=1}^{m_i} w_{sc_{i,k}}}}\right)^2}{l}} \tag{22}$$

where m_i is the number of subcategories for the main category i. For method 3 we obtain:

$$\widehat{\sigma}_{\overline{\overline{w}}_{sc_{i,j}}} = \sqrt{\frac{\sum_{k=1}^{l}\left(f_i\left(\widetilde{w}_{sc_{i,j_k}} - w_{sc_{i,j}}\right)\right)^2}{l}} \tag{23}$$

where the parameter c_i is given in eq. 13.

The second things that differs between the weighting methods is that the scaling parameter a varies between the methods (see eq. 14).

3.6. Using suitability mapping for localisation

The normalized suitability raster can also be thought of as an inverse of a cost surface. Cost surfaces are rasters in which higher cell values indicate higher cost for example in a pathfinding analysis (Collischonn and Pilar, 2000). By subtracting the normalized suitability raster from 1, we can use traditional pathfinding algorithms to find a least cost path regarding ground conditions. For each method (M1, M2 and M3), two sets of paths were searched, one unconstrained search covering the whole area and one constrained within the suggested corridors found working material for the localization study for embankment rail made by the Swedish Transport Administration. Obstacles such as villages, lakes, quarries and cities were masked out from the cost surface except for a buffer zone by existing rail in the cases of populated areas. The python package Scikit-image was used for the least cost path analysis in native resolution (10 × 10). The tool "route_through_array" uses a variation of Dijkstra's algorithm that finds a path that minimizes cumulative cost while also considering a geometric factor, balancing the

total cost with path directness.

To test the different normalisation approaches and compare against a traditional approach to line selection, pier foundations have been evaluated along the found paths according to a set of standardized foundation classes optimized for an industrial production (Table 4). The pier locations were found by optimising the total suitability sum within the least cost paths in 40-m sets according to the bridge elements. The reference line was developed by Skanska Sweden by means of traditional line selection methodology.

4. Results

4.1. Expert interviews

All judgement matrices were successfully filled out with a consistency below 0.1. The final judgement matrix for the main category was filled out during a discussion session with all experts and the final agreed upon matrix was consistent (CR < 0.01). The main category consensus matrix and the subcategory aggregated matrices are presented in the appendix.

Pearson correlation coefficients were calculated between each pair of expert judgments for the subcategories, with values closer to 1 indicating stronger agreement and values closer to -1 indicating stronger disagreement. A varying degree of consensus across the six subcategories was observed. Rock type shows the highest average correlation and the narrowest range, indicating the strongest consensus among experts for this category (excluding one expert who provided no answer). Slope and soil depth showed the second and third highest overall agreement. Soil type demonstrated good agreement. Wetness index opinions were divided, with four experts in strong agreement and one expert disagreeing. Groundwater occurrence showed the most diverse opinions, with both strong positive and negative correlations observed. Notably, two experts provided invariant judgments for the groundwater occurrence subcategory, and one expert each for the wetness index and rock type subcategory. Table 5 summarizes these findings.

Table 5
Pearsons's correlation coefficients for each pair of judgments for all subcategories within the main categories.

Sub category	Range	Avg. Correlation	Notes
Rock Type	0.98–1.00	0.99	Highest agreement, one expert with no variation
Slope	0.43–0.96	0.85	Very high overall agreement
Soil Depth	0.24–0.99	0.79	Strong agreement, one outlier
Soil Type	0.41–0.91	0.75	Good overall agreement
Wetness index	−0.57-0.95	0.41	Divided opinions
Groundwater occurence	−0.64-0.97	0.14	Most diverse opinions

4.2. Weight setting

Based on eq. 5 and the result from the expert group, the weights for the main categories in Table 6 were obtained. The soil type category is weighted highest while the rock type is assigned the lowest weight.

Soil type is weighted as the most influential parameter for ground suitability. The depth of the soil type layers is also weighted high while the remaining categories are weighted roughly equal and low.

The normalized weights for each sub-category and method are presented in Fig. 2. The M1 weights are relatively similar. Soil type and soil depth have the highest weights followed by slope and rock type. For the two groundwater related categories, only dry conditions and low-capacity fracture aquifers are weighted at a substantial contribution level. M2 decreases the overall contribution of rock type and aquifer capacity. Soil type increases in weight while soil depth and slope remain relatively unaltered. In M3 all contributions by categories other than soil depth and soil type are reduced in contribution to the overall suitability. All methods favour outcrops, low soil depths, glacial tills and coarse-grained sediments. M1 and M2 also suggest a significant contribution to suitability by low angle slopes while M3 does not. The most frequently occurring and highly rated criteria is coarse grained glacial tills.

Table 6
Weights for the main categories.

Soil type	Soil depth	Rock type	Wetness index	Slope	Groundwater occurrence
0.40	0.22	0.08	0.11	0.10	0.10

4.3. Suitability maps

The suitability maps are composed of the sum of the normalized subcategory weights in each cell of the raster (Fig. 3). The closer to a score of 1, the higher the suitability. While in general, the suitability maps are similar in appearance, marked differences between normalisation methods exists. Notably, M1 suitability is more pronounced in favouring the northern half of the investigated area showing higher contrast between suitable and less suitable areas overall. The distributions of normalized suitability scores go from being roughly normally distributed for M1 to a higher frequency of higher suitability values in M2 and bimodal in M3. River valleys, areas with organic deposits, clay and urban areas as consistently deemed less suitable through all three methods. Likewise, outcrops are deemed highly suitable throughout all three methods. Areas with high soil depth visible in the southern part of the area (Fig. 1) consistently have a lower suitability score over all methods.

Although the maps showing normalized suitability are best presented on a continuous colour scale, the absolute differences may be hard to properly notice. Therefore, maps outlining the difference in normalized suitability between methods were constructed (Fig. 4). These difference maps employ a normalized difference index to highlight relative discrepancies between the suitability assessments. This index is calculated as:

Table 4
Foundation types and evaluation criteria developed by Skanska Sweden for dimensioning estimates during early-stage planning. Soil conditions are evaluated from effective angle of internal friction (φ'_k) and undrained shear strength ($c_{u,k}$).

Class	Type	Soil Condition	Slab Dimensions (m)	Concrete Volume (m^3)	Reinforcement (tons)	Piles
F1	Slab	Rock/Friction soil ($\varphi'_k \geq 40°$)	5.0 × 8.0 × 1.2	48	6	–
F2	Slab	Friction soil ($\varphi'_k \geq 37°$)	6.0 × 9.0 × 1.4	76	9	–
F3	Slab	Friction soil ($\varphi'_k \geq 35°$)	7.0 × 10.0 × 1.6	112	12	–
F4	Slab	Friction soil ($\varphi'_k \geq 32°$)	8.0 × 11.0 × 1.8	159	18	–
F5	Pile	Very low-strength soil/Clay ($c_{u,k} \geq 20$ kPa)	7.0 × 10.0 × 1.8	126	14	48 × P270-4fi20 or fi170 × 12.5
F6	Pile	Clay ($c_{u,k} \geq 10$ kPa)	8.0 × 11.0 × 2.0	176	20	36 × P350-8fi20 or fi270 × 12.5
F7	Pile	Clay/Peat ($c_{u,k} \geq 5$ kPa)	9.0 × 13.0 × 2.2	258	28	48 × P350-8fi20 or fi270 × 12.5

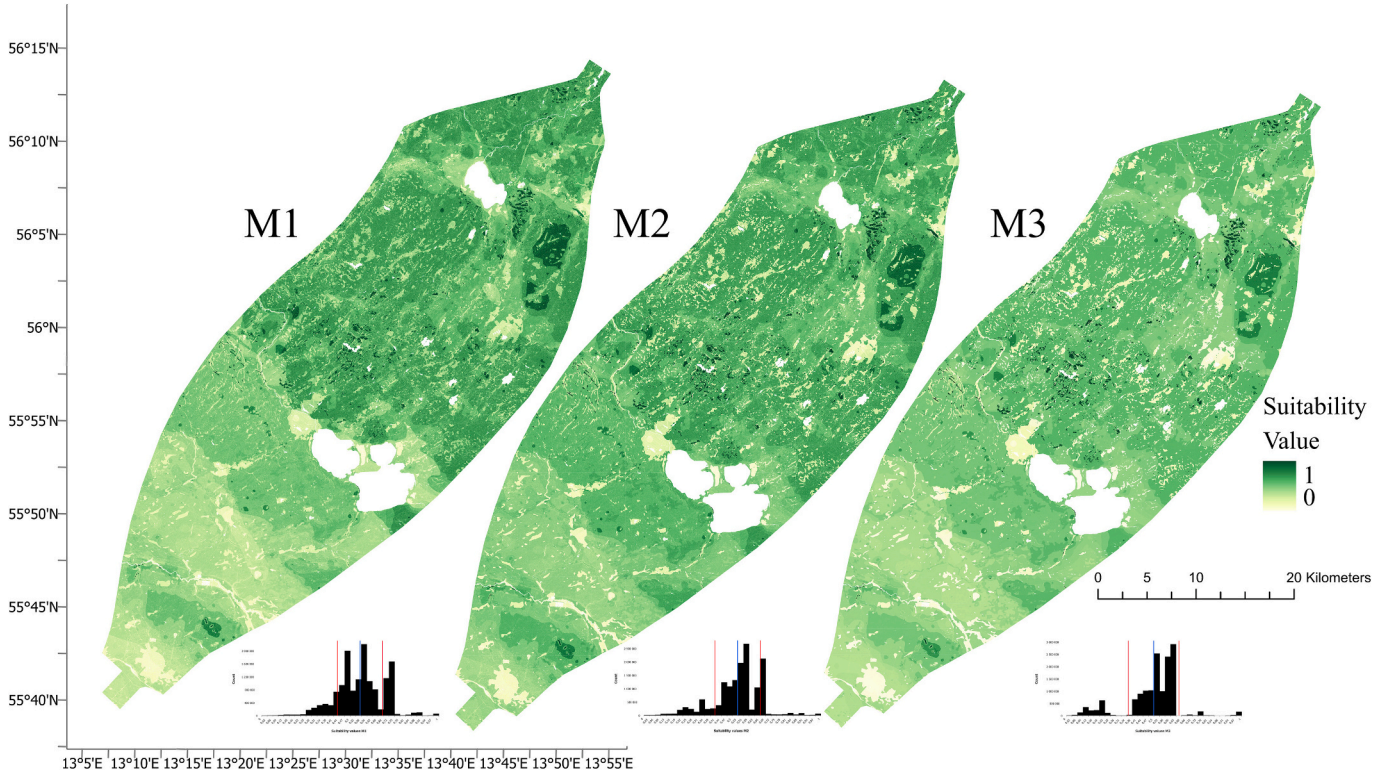

Fig. 3. Comparison of final suitability of ground conditions for pier foundation construction between methods M1-M3 and their normalized weight distribution (y: count, x: suitability value 0–1). The red vertical lines in the distribution plot shows the quartile bounds. Note the distinct decoupling of low normalized suitability values in the distribution of M3. (For interpretation of the references to colour in this figure legend, the reader is referred to the web version of this article.)

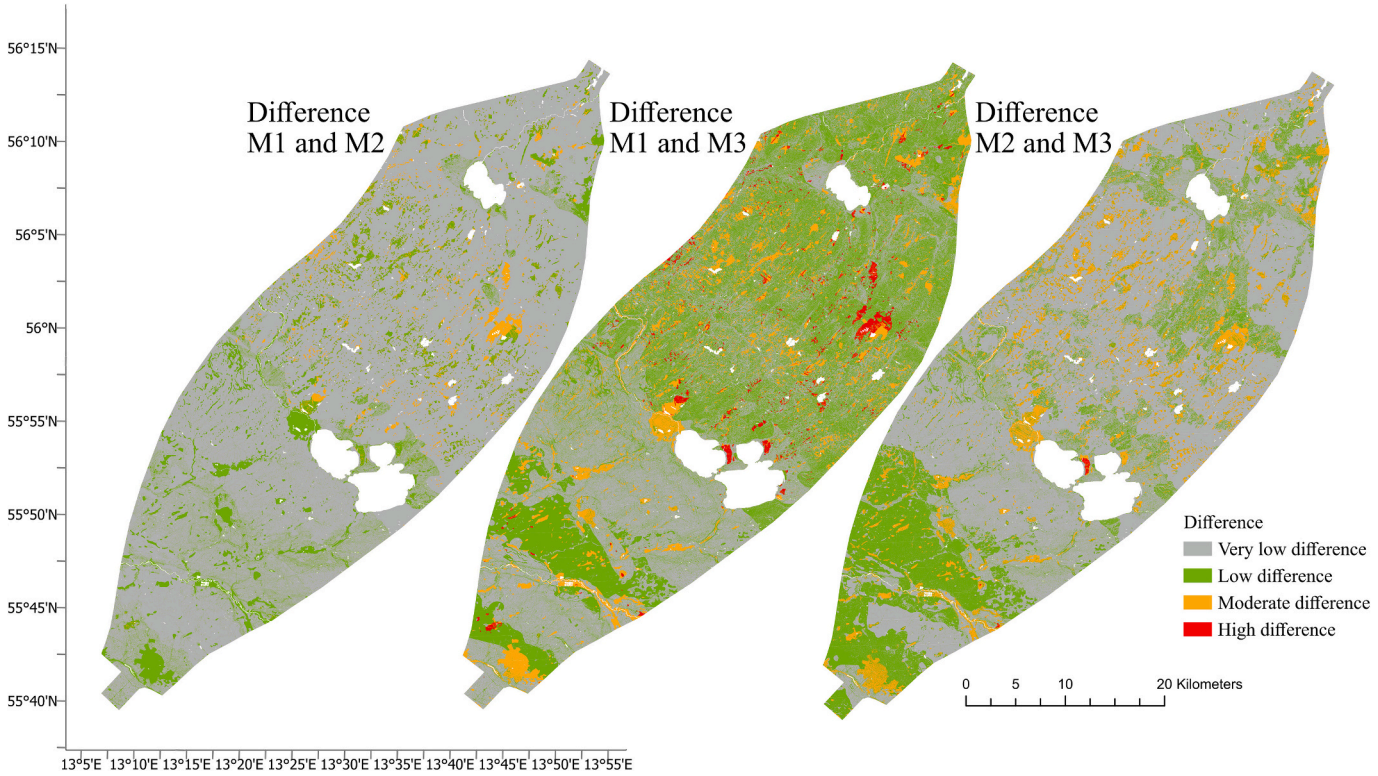

Fig. 4. Difference maps between methods M1-M3.

This approach produces values ranging from 0 % (identical values) to nearly 200 % (maximum possible difference between normalized values). While this range extends beyond the typical 0–100 % scale, it effectively captures the full spectrum of possible differences. To aid interpretation, the results were classified into four categories:

0–10 %: Very low difference.

$$\text{Normalized Difference Index} = (|\text{Raster1} - \text{Raster2}|/((\text{Raster1} + \text{Raster2})/2)) \times 100$$

10–40 %: Low difference.

40–100 %: Moderate difference.

100–200 %: Very high difference.

This approach allows for highlighting even extreme differences between the two normalized suitability assessments, with values over 100 % indicating cases where one assessment shows high suitability while the other shows low suitability for the same area.

The difference maps show a large difference in normalized suitability between M1 and M3 while differences between M1 and M2 are negligible. The largest differences between M1 and M3 is the normalized suitability on regions of organic sediments (Fig. 4). These sediments are deemed less suitable in M3 than in M1, with some variation for smaller differences in other categories. The moderate to high difference between M1 and M3 can, in most cases, be traced to such organic sediments, but also made ground, where made ground on shallow soil depths are more suitable in M1 than in M3. The low difference spectrum (green colour) is, in most cases, caused by a slightly lower suitability of fine grained and coarse-grained glacial tills of low to moderate soil depth in M3 compared to M1. The only high difference between M2 and M3 can be traced to an area of high soil depth and consisting of organic sediments where M3 display a much lower normalized suitability than M2. Moderate differences are due to a slightly higher suitability of organic sediments and sorted fine grained sediments on low soil depths in M2 compared to M3. Low differences between M2 and M3 are due to a variety of factors in slight differences of slope, soil depth and mainly sorted coarse grained sediments and fine-grained glacial tills.

4.4. Uncertainty maps

The uncertainty of the suitability score for each method is visualized in Fig. 5. Highest overall uncertainty is observed in M1 and the lowest in M2. M1 uncertainties are relatively normally distributed, but a separate concentration of high uncertainty values is present. M2 and M3 display a more scattered distribution with a larger concentration in the higher range. All three methods agree on higher uncertainties in areas with higher suitability and vice versa. Outcropping bedrock and flat areas with low soil depth and glacial till are responsible for most of the high uncertainty areas which also corresponds to areas with high suitability. Similarly, areas of high soil depth, river valleys, peatland and clay areas have low uncertainty, and low suitability, throughout all three methods.

4.5. Localisation

For both the constrained and unconstrained search, the found paths between the three normalisation methods are largely the same (Fig. 6). The differences lie in the details, but follow the general pattern outlined in Fig. 2, where M3 steers more heavily towards outcrops and coarse-grained soils than M1 which smooths that preference for lesser slopes or changes in bedrock.

The foundation type distribution across the found paths and pier positions relative to each normalisation approach and the reference line is presented in Fig. 7a for the unconstrained search pattern. The percentage of non-piled foundation classes for the AHP approach is above 90 % for all three normalisation methods. The reference line yields 84.1 % of non-slab foundations, although a majority of the slabs are of type F4, meaning high concrete and steel tonnages. The constrained paths are similar to the unconstrained in relative distribution of foundation classes but finds less optimal foundation conditions (F1) due to the limited search area (Fig. 7b).

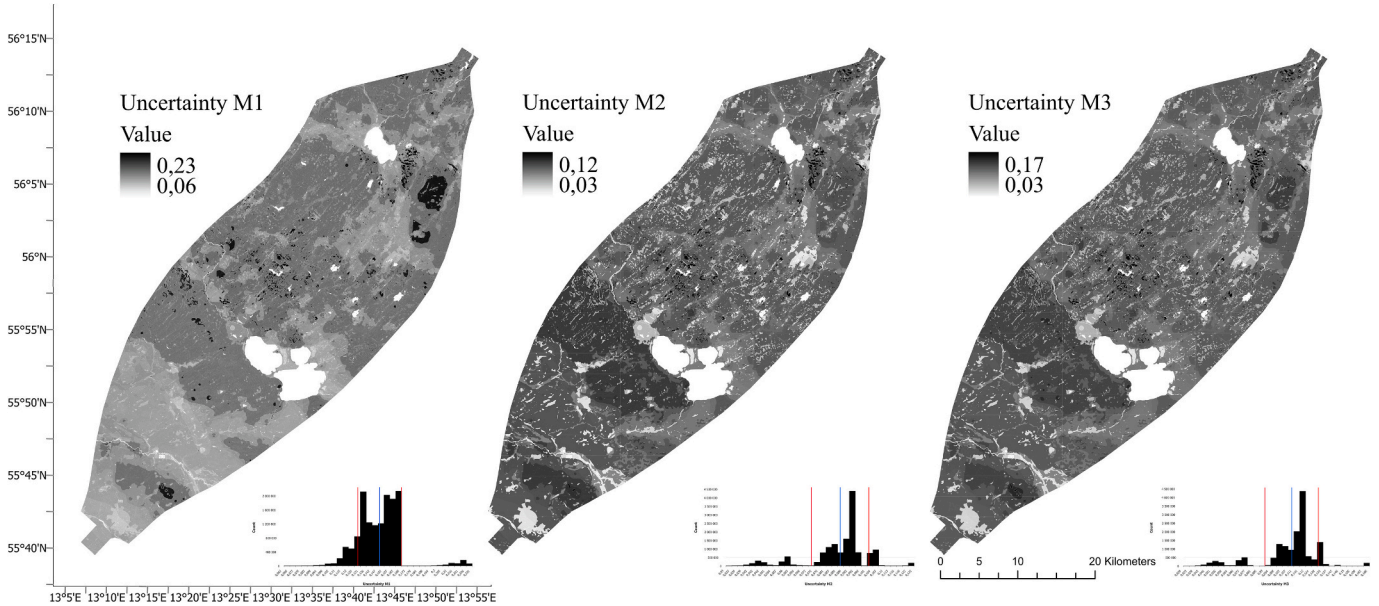

Fig. 5. Uncertainty maps displaying the propagated uncertainty of pairwise comparisons for each method.

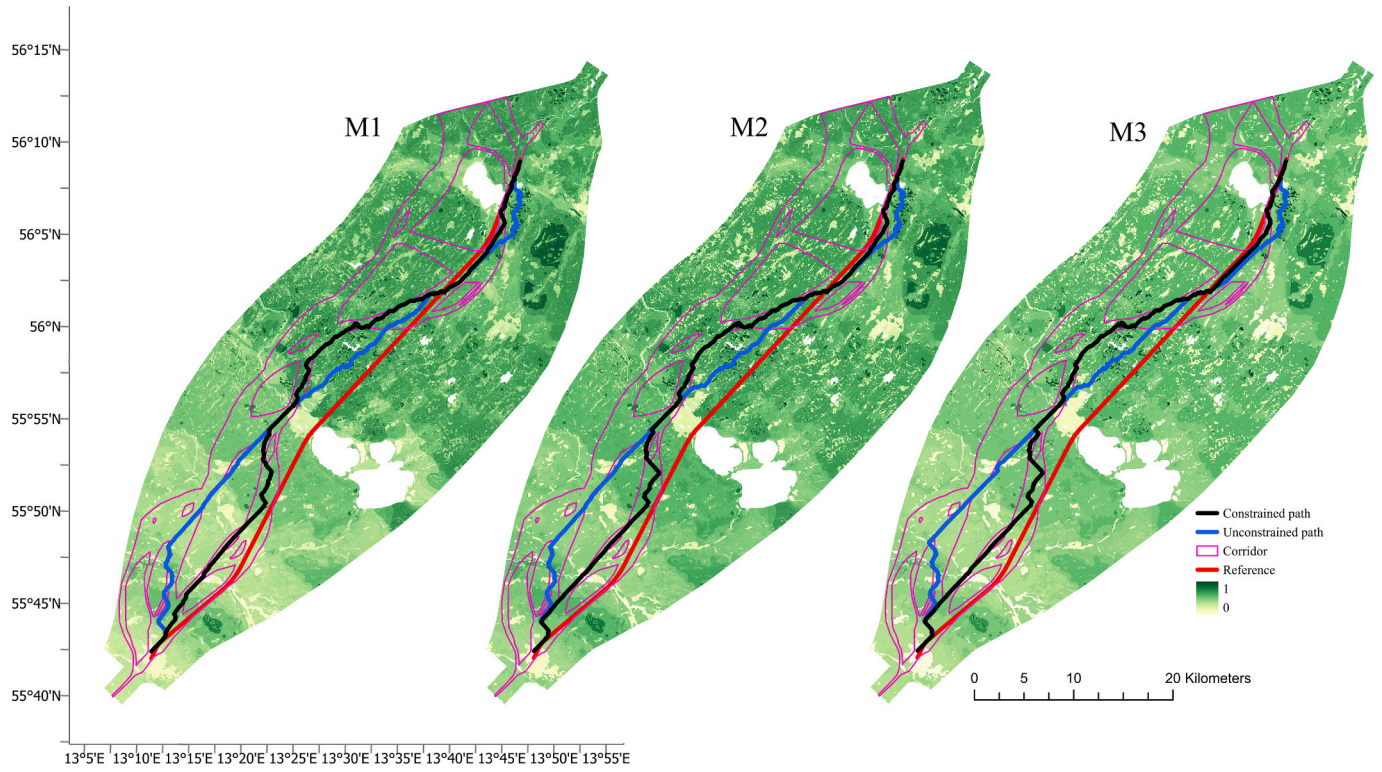

Fig. 6. Least cost paths found using M1-M3 cost rasters in a constrained and unconstrained search pattern. The red line outlines the reference line. The constraint is outlined in the figure as the corridor. (For interpretation of the references to colour in this figure legend, the reader is referred to the web version of this article.)

5. Discussion

5.1. Selection of categories and expert assessment

The selection of relevant evaluation categories is an essential part of developing meaningful analysis outcomes. The six categories employed in this study were selected by and subdivided due to their individual contributions to the construction of pier foundations. The extended geological mapping in the area also contributed to reliability of the chosen categories and subdivisions. If the method is applied to areas where no extended geological mapping is conducted, other subdivisions may have to be made. Similarly, the selected categories need to be adapted to the local geology for each unique site.

Analysis of the correlation matrices from expert judgments revealed notable patterns in category assessment reliability. Groundwater-related criteria, specifically aquifer characteristics and soil moisture indices, showed lower inter-expert agreement and higher instances of invariant judgement. This pattern suggests potential limitations in these categories' relevance or effectiveness for the intended analysis, further emphasized by their relatively low normalized weights and minimal contribution to overall suitability assessments. While groundwater conditions are widely recognized as crucial in engineering projects (Knutsson and Morfeldt, 1993; Kolat et al., 2006), the indirect representation through aquifer potential and wetness indices appeared to impede meaningful expert evaluation. Although the main category discussions achieved consensus, future applications would benefit from extending consensus discussions to subcategory levels to ensure more robust expert judgments. The pairwise comparison process may however be subject to inattentive expert judgments as the number of pairwise comparisons grow (Tavana et al., 2023).

The methodology could be enhanced through the incorporation of additional data sources, where available:

- Direct groundwater level measurements
- Three-dimensional stratigraphic models
- Cone penetration test (CPT) results

In particular, incorporating actual groundwater level data could provide a more direct and meaningful metric for engineering evaluation compared to the current proxy indicators. Similarly, where 3D geological models exist, stratigraphic complexity could be quantified and integrated into the pairwise comparison framework. CPT data covering major terrain types could facilitate both more precise soil type classification and direct integration into the judgement matrix.

During the discussions filling in the judgement matrix for the main criteria, the issue of local expertise came up. Participants were showed the distribution of the judged criteria in the study area to get a complete picture of the mapped ground conditions. The experts are based in different parts of the country and have different local knowledge of ground conditions in the study area. These differences became evident while discussing for example soil types and rock types. A very prevalent soil type in the study area is variations of fine-grained glacial tills which are sparse in other parts of the country. The over consolidated nature and loading strength of such tills are not widely known in areas where the soil type does not exist. Likewise, sedimentary rock types are uncommon in other parts of the country, explaining why the differences in geotechnical behaviour of sedimentary and the more common crystalline rocks required some discussions to be resolved. A point, over-looked during the discussion was the specific nature of the local coarse-grained tills. In much of Sweden, these tills are typically thought of as subglacial deposits and highly consolidated. The local geology however shows a greater prevalence for melt out tills which are less consolidated. The fact that sorted coarse grained material is weighted the same as coarse grained tills do however suggest a compounded experience-based weighting from the experts. Such discussions and results highlight the need for local knowledge of ground conditions and site-specific judgement in favour of general classifications.

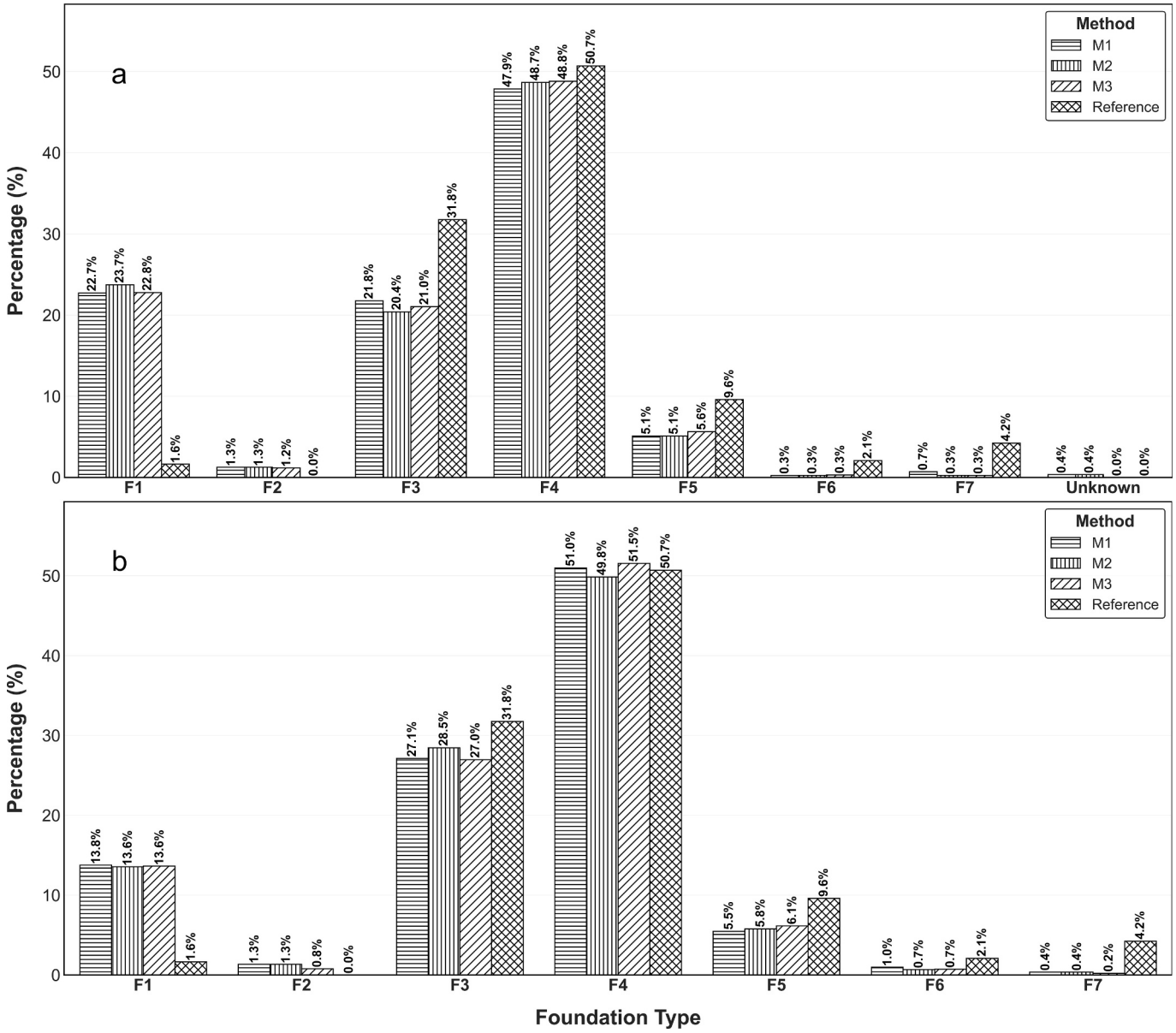

Fig. 7. Assigned foundation classes (F1-F7) based on (a) unconstrained least cost path and (b) constrained least cost path over the suitability rasters M1-M3 and a reference line from traditional line localisation. Unknown foundation types arises when unclassified ground conditions are traversed. The low amount of F2 foundation classes is due to the local geology being poor in thick very coarse-grained friction soils.

5.2. Weighting methods for the subcategories

Which of the methods is best to compute the weights for the features on subcategory level $\left(w^{rs}_{t_{i,j}}, \overline{w}^{rs}_{t_{i,j}} \text{ or } \overline{\overline{w}}^{rs}_{t_{i,j}}\right)$ depends on how the experts think when they decide the pairwise relationship in the AHP process. If they base their decision on the importance of each main category, irrespective of the number of classes in the main category, then $\left(\overline{w}^{rs}_{t_{i,j}}\right)$ would be reasonable to use. If they also include local knowledge of the distribution of features into their pairwise relationship it could be better to use the $\left(\overline{\overline{w}}^{rs}_{t_{i,j}}\right)$ weights. The rationality is that they include the effect of the local distribution of the features in their judgement of the importance when they judge the pairwise relationships in the AHP process (cf. the section on M3 weights for the slope category in 3.4.2 for further details).

The three methods used here all emphasise the importance of suitable soil types such as the over-consolidated fine-grained tills, sorted coarse grained material and the coarser melt-out tills as well as no soil cover at all. All methods are also in agreement that shallow soil depths are preferable. In M1 however, most categories are of similar importance, although with a broad span of weights in the subcategories. M2 relieves the rock type of high importance and the overall contribution to suitability decreases due to adjustment of matrix size. M3 further enhances this effect and the difference between sedimentary rock and crystalline rock also diminishes and the importance of soil type increases while having bigger differences between soil types than in M1. Soil thickness is kept rather similar between methods.

To summarise, M3 distils the suitability analysis to be about soil types and soil depth. M2 also highlights slope as an important factor and M1 keeps the crystalline rocks as an important factor in ground suitability. None of the methods highlights the two parameters wetness index and groundwater occurrence as important factors.

A case can be made to consistently employ all three methods of normalisation to diversify the outcomes of the use cases of the suitability assessment. In this example, if foundation types are only evaluated based on soil type and soil depth, M3 is preferred over the other methods due to its heavy reliance on these categories. If slope and rock type are part of construction codes for foundations, M1 would better reflect the sought-after conditions.

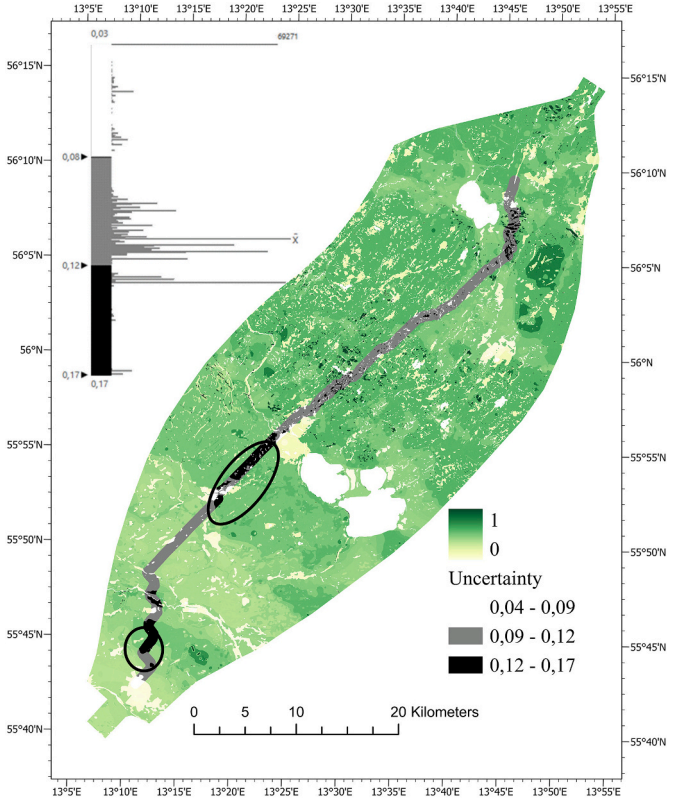

Fig. 8. Areas of high uncertainty and high to moderate suitability highlighted for the M3 paths in unconstrained search. The histogram shows the data division for colour coding. Areas of high suitability and high uncertainty are highlighted where a significant stretch of the line is found under these conditions.

5.3. Uncertainty maps

Figure 5 illustrates the uncertainties for the three methods. It should be emphasized that the uncertainties shown are only the result of how the uncertainties in the input data (taken from the judgement matrices in the AHP method generated by the experts) propagate in the computations. This implies that what the uncertainty maps show are the uncertainty in the estimations under the assumption that the weights are correct. Of course, as illustrated in other parts of this paper, there are also uncertainties in the weights that needs to be considered if a total uncertainty should be estimated. This implies the following:

2) It is not possible to state that one weighting method is better than another one only on basis that it has lower uncertainty values.
3) For total uncertainty estimations a combination of the uncertainty in the propagation of the uncertainty in the input data (given in Fig. 5) and the uncertainty in the weight setting (which is indicated in Fig. 4) is needed.

However, these uncertainty maps provide valuable guidance for identifying areas of high suitability but uncertain classification - critical information for field investigation planning. Areas with high agreement on suitability may require fewer resources for investigation, while areas of agreed-upon low suitability warrant intensive field investigation. Areas showing high suitability, but significant uncertainty represent priority targets for detailed investigation.

Figure 8 demonstrates practical application of uncertainty estimates, highlighting areas of high uncertainty and moderate-to-high suitability along the M3-derived path. These highlighted regions, characterized by varying fine-grained glacial tills and moderate soil depths overlying sedimentary bedrock, represent priority areas for detailed investigation based on expert input divergence.

It is important to note that inherent data uncertainty, particularly regarding spatial accuracy of source datasets, falls outside this study's scope, as the methodology focuses on early-stage planning using openly available data. Spatial accuracy is expected to improve with project-specific data acquisition in later project stages.

5.4. Localisation

The pathfinding analysis results, together with predefined evaluation criteria progressing from simple to complex foundation classes, demonstrate clear preference for simpler slab foundations across all normalisation methods. This alignment between AHP-derived paths and simpler foundation requirements is particularly noteworthy given that the expert group focused primarily on construction ease rather than foundation complexity in their evaluations. While the raw least-cost paths produced by the algorithm require smoothing to achieve more realistic railway alignments, the advantage in simpler foundation classes

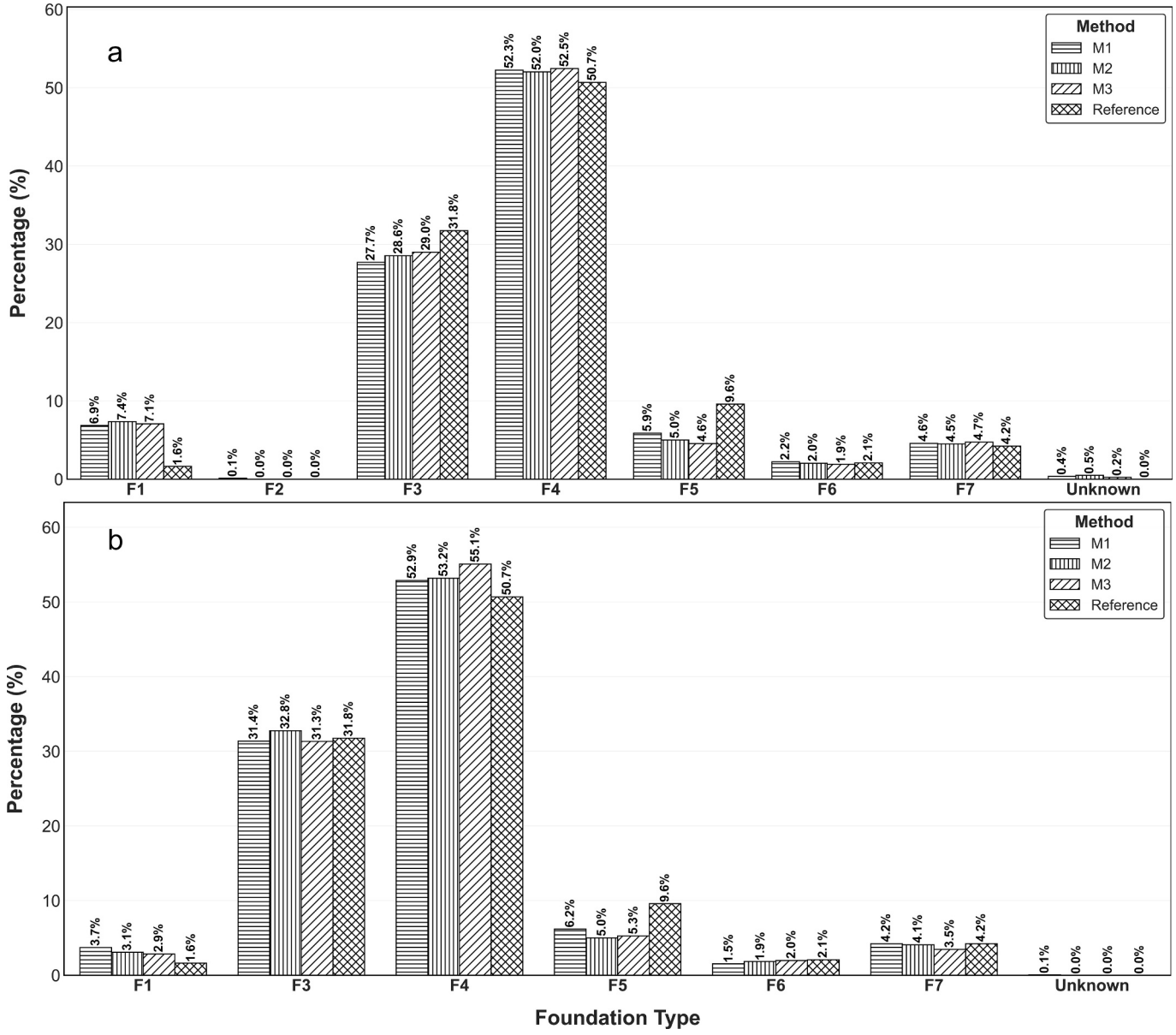

Fig. 9. Foundation classes after smoothing the least cost paths for (a) unconstrained and (b) constrained search spaces. The reference line remains the same. In (b), no F2 configuration was found and are therefore not shown in the diagram.

persists after smoothing, particularly in unconstrained path scenarios (Fig. 9).

It should be noted that the routes found in the pathfinding analysis are solely based on the cost rasters, except for masked out areas. For further research it is suggested to apply minimum curve radius constraints directly to the pathfinding algorithm specified for the planned speed. Random search methods have been shown to effectively handle such tasks (Pu et al., 2024). The elevation profile of the selected route will also play a major role in pier height and stretches of deviating foundation techniques such as bridge, tunnel and embankment. The routes presented here do not account for societal, archaeological and environmental constraints which ideally would be tested in conjunction with the presented methodology. Such data can be added as separate compounded layers following the same methodology or be part of a larger AHP.

6. Conclusions

The study demonstrates the potential of using MCA-AHP for ground suitability assessments in early-stage railway planning. By integrating expert judgments and testing three different weight normalisation methods, significant impact on suitability outcomes were highlighted. The results emphasise the importance of considering multiple approaches to weight normalisation, as each method prioritizes different aspects of ground conditions, such as soil type, depth, and slope. This flexibility allows planners to adapt the analysis based on specific project needs and expert perspectives.

Uncertainty mapping can be a valuable tool for identifying areas where suitability is uncertain, providing guidance for prioritizing field investigations. By focusing resources on areas of high suitability but high uncertainty, planners can enhance the efficiency of site investigations and reduce the risk of unforeseen ground conditions impacting project timelines and costs.

Since pointwise loading of the ground reduces the emphasis on mass balance calculations in early-stage planning, an alternative planning pipeline is required. The AHP approach, focusing on ground suitability for construction demonstrates good agreement in minimizing the complicated predefined foundation classes intended for an

industrialized approach to railway construction.

The case study between Lund and Hässleholm illustrates how the methodology can be applied in practice, offering a structured and transparent framework for comparing ground suitability across large areas. While the study focused on pier-supported viaduct railways, the approach is adaptable to other infrastructure projects requiring geotechnical evaluations. However, the method should not be viewed as static in terms of the expert judgments. Instead, it is important to emphasise that each unique region under investigation must carry out the steps of category selection and pairwise comparison based on the local geology and sediment deposition history.

In conclusion, the approach represents a practical step forward in early-stage infrastructure planning, providing robust tools for decision-makers to assess and mitigate geotechnical risks. Future research should explore the integration of additional data sources, such as 3D geological models, groundwater levels and stratigraphic information to further refine the analysis. Extending the approach to consider environmental and socio-economic factors, topography and maximum curvature alongside geological suitability is encouraged in railway route localisation.

CRediT authorship contribution statement

Joakim Robygd: Writing – original draft, Visualization, Investigation, Formal analysis. **Lars Harrie:** Writing – original draft, Methodology, Formal analysis. **Tina Martin:** Writing – review & editing, Supervision.

Declaration of competing interest

The authors declare that they have no known competing financial interests or personal relationships that could have appeared to influence the work reported in this paper.

Acknowledgements

The work was carried out within the framework of the Infra-Sweden2030/Vinnova project “REICOR - Rational and efficient ground investigations for industrialised construction of new railways” (project 2022 00188) which is funded by Vinnova, Formas, Energimyndigheten, SBUF (project 13996), Trafikverket (project TRV2019/70975), Skanska, Swedish Geological Survey, Lund University and Uppsala University. The authors are grateful for the help of the assembled expert group that provided the pairwise comparison consisting of Mats Svensson, Lars O Ericsson, William Bjureland, Alfredo Mendoza, Ulf Håkansson, Johan Spross and Ola Forssberg.

Appendix A. Appendix

Total normalised weights per subcategorical level and method.

	Fine grained glacial tills	Coarse grained glacial tills	Sorted coarse grained material	Outcrops	Unknown (made ground)	Sorted fine grained material	Organic sediments	Open water
M1	0.19	0.16	0.19	0.30	0.02	0.02	0.00	−0.01
M2	0.33	0.29	0.33	0.50	0.06	0.05	0.03	0.01
M3	0.44	0.38	0.44	0.66	0.09	0.08	0.05	0.03

	0–3 m	3–11 m	11–24 m	24–46 m	>46 m
M1	0.3	0.12	0.05	0.01	−0.01
M2	0.28	0.12	0.04	0.01	−0.01
M3	0.3	0.13	0.05	0.01	−0.01

	Sedimentary bedrock	Crystalline bedrock
M1	0.02	0.13
M2	−0.03	0.01
M3	−0.04	−0.03

	Dry	Moist	Wet	Discharge
M1	0.08	0.05	0.01	−0.01
M2	0.03	0.01	−0.01	−0.03
M3	−0.02	−0.03	−0.03	−0.04

	0–5°	5–10°	10–18°	>18°
M1	0.14	0.02	−0.01	−0.03
M2	0.11	0.01	−0.02	−0.03
M3	−0.01	−0.04	−0.04	−0.04

	Fracture aquifer small	Fracture aquifer large	Porous aquifer small	Porous aquifer large
M1	0.06	0.02	0.05	0.02
M2	0.02	−0.01	0.01	−0.01
M3	−0.02	−0.03	−0.02	−0.03

Data availability

Data will be made available upon reasonable request.

References

Adiat, K.A.N., Nawawi, M.N.M., Abdullah, K., 2012. Assessing the accuracy of GIS-based elementary multi-criteria decision analysis as a spatial prediction tool - a case of predicting potential zones of sustainable groundwater resources. J. Hydrol. 440–441, 75–89. https://doi.org/10.1016/j.jhydrol.2012.03.028.

Andersson-Sköld, Y., Bergman, R., Johansson, M., Persson, E., Nyberg, L., 2013. Landslide risk management - a brief overview and example from Sweden of current situation and climate change. Int. J. Disaster Risk Reduct. 3 (1), 44–61. https://doi.org/10.1016/j.ijdrr.2012.11.002.

Anjar, J., Larsen, N.K., Håkansson, L., Möller, P., Linge, H., Fabel, D., Xu, S., 2013. A 10Be-based reconstruction of the last deglaciation in southern Sweden. Boreas 43 (1), 132–148. https://doi.org/10.1111/bor.12027.

Bathrellos, G.D., Skilodimou, H.D., Chousianitis, K., Youssef, A.M., Pradhan, B., 2017. Suitability estimation for urban development using multi-hazard assessment map. Sci. Total Environ. 575, 119–134. https://doi.org/10.1016/j.scitotenv.2016.10.025.

Baynes, F.J., Fookes, P.G., Kennedy, J.F., 2005. The total engineering geology approach applied to railways in the Pilbara, Western Australia. Bull. Eng. Geol. Environ. 64 (1), 67–94. https://doi.org/10.1007/s10064-004-0271-4.

Bell, F.G., Cripps, J.C., Culshaw, M.G., O'Hara, M., 1987. Aspects of geology in planning. In: Culshaw, M.G., Bell, F.G., Cripps, J.C., O'Hara, M. (Eds.), Planning and Engineering Geology. Geol. Soc. Eng. Geol. Spec. Publ., vol. 4, pp. 1–38. https://doi.org/10.1144/gsl.eng.1987.004.01.01.

Collischonn, W., Pilar, J.V., 2000. A direction dependent least-cost-path algorithm for roads and canals. Int. J. Geogr. Inf. Sci. 14 (4), 397–406. https://doi.org/10.1080/136588100500243O4.

Costa, A.N., Polivanov, H., Alves, M.G., Ramos, D.P., 2011. Multicriterial analysis in the investigation of favorable areas for edifications with shallow and deep foundations in the Municipality of Campos dos Goytacazes - Rio de Janeiro, Brazil. Eng. Geol. 123 (3), 149–165. https://doi.org/10.1016/j.enggeo.2011.05.011.

Delmonaco, G., Leoni, G., Margottini, C., Puglisi, C., Spizzichino, D., 2003. Large scale debris-flow hazard assessment: a geotechnical approach and GIS modelling. Nat. Hazards Earth Syst. Sci. 3, 443–455. https://doi.org/10.5194/nhess-3-443-2003.

Deng, F., Pu, J., Huang, Y., Han, Q., 2023. 3D geological suitability evaluation for underground space based on the AHP-cloud model. Underground Space 8, 109–122. https://doi.org/10.1016/j.undsp.2022.03.006.

Dueck, A., 1998. Shear Strength and Matric Suction in Clay Tills - Triaxial Test Procedures to Evaluate Shear Strength of Clay Tills from Southwestern Sweden. Diss. Lund Inst. Technol., Lund Univ., Dep. Geotechnol., Lund.

Elsheikh, R., Mohamed Shariff, A.R.B., Amiri, F., Ahmad, N.B., Balasundram, S.K., Soom, M.A.M., 2013. Agriculture Land Suitability Evaluator (ALSE): a decision and planning support tool for tropical and subtropical crops. Comput. Electron. Agric. 93, 98–110. https://doi.org/10.1016/j.compag.2013.02.003.

Fernández, D.S., Lutz, M.A., 2010. Urban flood hazard zoning in Tucumán Province, Argentina, using GIS and multicriteria decision analysis. Eng. Geol. 111 (1–4), 90–98. https://doi.org/10.1016/j.enggeo.2010.06.006.

Fookes, P.G., Baynes, F.J., 2001. Total geological history: a model approach to understanding site conditions. Ground Eng. March 2001, 28–31.

Government Office of Sweden, 2023. Uppdrag att planera för åtgärder i järnvägssystemet i Skåne samt ändring av den nationella trafikslagsövergripande planen för transportinfrastrukturen för perioden 2022–2033. Government Decision 2023-10-26.

Griffiths, J.S., 2017. Terrain evaluation in engineering geology. Q. J. Eng. Geol. Hydrogeol. 50 (1), 3–11. https://doi.org/10.1144/qjegh2016-090.

Huang, R.Q., Li, Y.R., Qu, K., Wang, K., 2013. Engineering geological assessment for route selection of railway line in geologically active area: a case study in China. J. Mt. Sci. 10 (4), 495–508. https://doi.org/10.1007/s11629-013-2660-2.

Ising, J., Bergström, U., Erlström, M., Grigull, S., Malmberg Persson, K., Wickström, L., Lundqvist, L., Engdahl, M., 2019. Hässleholm-Lund - uppgraderad geologisk information inför projektering av höghastighetsjärnväg. SGU-rapport 2019:03.

Ishak, A., Asfriyati, Akmaliah, V., 2019. Analytical hierarchy process and PROMETHEE as decision-making tool: a review. IOP Conf. Ser.: Mater. Sci. Eng. 505 (1), 012085. https://doi.org/10.1088/1757-899X/505/1/012085.

Jain, A.K., 2010. Data clustering: 50 years beyond K-means. Pattern Recogn. Lett. 31 (8), 651–666. https://doi.org/10.1016/j.patrec.2009.09.011.

Joshi, N., Lund, B., Roberts, R., 2024. Probabilistic seismic hazard assessment of Sweden. Nat. Hazards Earth Syst. Sci. 24 (11), 4199–4223. https://doi.org/10.5194/nhess-24-4199-2024.

Karlson, M., Karlsson, C.S.J., Mörtberg, U., Olofsson, B., Balfors, B., 2016. Design and evaluation of railway corridors based on spatial ecological and geological criteria. Transp. Res. Part D Transp. Environ. 46, 207–228. https://doi.org/10.1016/j.trd.2016.03.012.

Knutsson, G., Morfeldt, C.-O., 1993. Grundvatten teori & tillämpning. AB Svensk Byggtjänst.

Kolat, Ç., Doyuran, V., Ayday, C., Süzen, M.L., 2006. Preparation of a geotechnical microzonation model using Geographical Information Systems based on multicriteria decision analysis. Eng. Geol. 87 (3), 241–255. https://doi.org/10.1016/j.enggeo.2006.07.002.

Koyama, Y., 1997. Railway Technology Today 1. Railway construction in Japan. Jpn. Railw. Transp. Rev. 14, 36–41.

Krejčí, J., Stoklasa, J., 2018. Aggregation in the analytic hierarchy process: why weighted geometric mean should be used instead of weighted arithmetic mean. Expert Syst. Appl. 114, 97–106. https://doi.org/10.1016/j.eswa.2018.06.060.

Larsson, R., 1989. Hållfasthet i friktionsjord. SGI Inform. 8.

Larsson, R., 2000. Lermorän – en litteraturstudie. Förekomst och geotekniska egenskaper. Statens Geotekniska Institut, Varia, p. 480.

Larsson, R., 2001. Investigations and Load Tests in Clay till. Results from a Series of Investigations and Load Tests in the Test Field at Tornhill outside Lund in Southern Sweden. Statens Geotekniska Institut, Rep, p. 59.

Malmborg, S.B., 1983. Packad lermoräns hållfasthets- och kompressionsegenskaper. Diss. Lund Inst. Technol., Lund Univ., Dep. Geotechnol., Lund.

Marchesini, I., Althuwaynee, O., Santangelo, M., et al., 2024. National-scale assessment of railways exposure to rapid flow-like landslides. Eng. Geol. 332, 107474. https://doi.org/10.1016/j.enggeo.2024.107474.

Nie, R., Chen, Y.F., Leng, W., Yang, Q., 2017. Experimental measurement of dynamic load parameters for pier pile caps of high-speed railway bridges. Proc. Inst. Mech. Eng. Part F J. Rail Rapid Transit 231 (2), 162–174. https://doi.org/10.1177/0954409715622965.

Nowell, D.A.G., 2021. Geology of Marseilles to Italy high-speed TGV railway line compared to HS2 in Britain. Geol. Today 37 (1), 23–30. https://doi.org/10.1111/gto.12338.

Pu, H., Wan, X., Song, T., Schonfeld, P., Peng, L., 2024. A 3D-RRT-star algorithm for optimizing constrained mountain railway alignments. Eng. Appl. Artif. Intell. 130, 107770. https://doi.org/10.1016/j.engappai.2023.107770.

Ringberg, B., 1992. Beskrivning till jordartskartan Kristianstad NV. Geol. Surv. Swed. SGU Ser. Ae, p. 111.

Saaty, R.W., 1987. The analytic hierarchy process-what it is and how to use it. Math. Model. 9 (5), 161–176. https://doi.org/10.1016/0270-0255(87)90473-8.

Saaty, T.L., 2008. Decision making with the analytic hierarchy process. Int. J. Serv. Sci. 1 (1), 83–98. https://doi.org/10.1504/IJSSCI.2008.017590.

SGI, 2016. Geokalkyl 2.0: Metodbeskrivning Och Implementering, 33. SGI Publ.

Shi, C., Wei, B., Wei, S., et al., 2021. A quantitative discriminant method of elbow point for the optimal number of clusters in clustering algorithm. Eur. J. Wireless Commun. Netw. 2021, 1–9. https://doi.org/10.1186/s13638-021-01910-w.

Skilodimou, H.D., Bathrellos, G.D., Chousianitis, K., et al., 2019. Multi-hazard assessment modeling via multi-criteria analysis and GIS: a case study. Environ. Earth Sci. 78 (2). https://doi.org/10.1007/s12665-018-8003-4.

Stroeven, A.P., Hättestrand, C., Kleman, J., et al., 2016. Deglaciation of Fennoscandia. Quat. Sci. Rev. 147, 91–121. https://doi.org/10.1016/j.quascirev.2015.09.016.

Su, M., Dai, G., Marx, S., et al., 2019. A brief review of developments and challenges for high-speed rail bridges in China and Germany. Struct. Eng. Int. 29 (1), 160–166. https://doi.org/10.1080/10168664.2018.1456892.

Swedish Transport Administration, 2018. Metodbeskrivning - Geokalkyl Infrastruktur, tidiga skeden.

Tavana, M., Soltanifar, M., Santos-Arteaga, F.J., 2023. Analytical hierarchy process: revolution and evolution. Ann. Oper. Res. 326, 879–907. https://doi.org/10.1007/s10479-021-04432-2.

Yalcin, M., Kilic Gul, F., 2017. A GIS-based multi-criteria decision analysis approach for exploring geothermal resources: Akarcay basin (Afyonkarahisar). Geothermics 67, 18–28. https://doi.org/10.1016/j.geothermics.2017.01.002.

Glossary

AHP: Analytical Hierarchy Process
CR: Consistency Ratio
GIS: Geographic Information System
MCA: Multi Criteria Analysis